Mountain Torques Caused by Normal-Mode Global Rossby Waves, and the Impact on Atmospheric Angular Momentum

HARALD LEJENÄS

Department of Meteorology, Stockholm University, Stockholm, Sweden

ROLAND A. MADDEN

National Center for Atmospheric Research, Boulder, Colorado*

(Manuscript received 8 October 1998, in final form 14 June 1999)

ABSTRACT

Planetary-scale free Rossby waves present in the earth's atmosphere propagate toward the west. Pressure torques varying in time then arise as a consequence of unequal pressure on the eastern and western sides of mountains and small-scale topographic features. These torques, referred to as mountain torques, have an influence on the exchange of angular momentum between the atmosphere and the earth.

The authors investigated the impact of all identified planetary-scale free Rossby waves on atmospheric angular momentum by computing the contribution from mountain torques to the rate of change of total atmospheric angular momentum for each wave.

Comparing contributions from individual waves, the authors found that for the average wave amplitudes the maximum torque for a particular wave is around 2 Hadleys, and that considering all meridional wavenumbers, zonal wavenumber 2 causes the largest global torques. Changes in angular momentum depend on both the amplitude of the changing torque and on its period. As a result zonal wavenumbers 1 and 2 cause the largest angular momentum anomalies with peak-to-trough amplitudes of 2–5 $\times$ 10^{23} kg m^2 s^{-1}. The 16-day wave produces the largest amplitude, 4.9 $\times$ 10^{23} kg m^2 s^{-1}. These values refer to average amplitudes reported in the literature. Individual waves may cause anomalies five times as big.

1. Introduction

Disturbances with structures that closely resemble normal-mode global Rossby waves are present in the earth's atmosphere. These waves are free waves, and their speeds and structures are determined by the resonant characteristics of the mean state of the atmosphere. The theoretical horizontal structures of these waves are given by Hough functions, which are the solutions of free waves in an atmosphere at rest (Hough 1898). Salby (1981a,b) showed that in the troposphere, even in the presence of realistic winds, the horizontal structures very much resemble Hough functions. Particular interest has been devoted to some of these global-scale oscillations, above all the 5-day wave and the 16-day wave. Several observational studies of these two waves have appeared in the literature. For instance, Deland (1964), Eliasen and Machenhauer (1965), Deland and Lin (1967), Madden and Stokes (1975), and Madden and Julian (1972) studied the 5-day wave. Characteristics of the 16-day wave have been examined by, for instance, Madden (1978) and Madden and Labitzke (1981).

Systematic studies of all kinds of planetary-scale free Rossby waves are also present in the literature. Dikii (1965), Golitsyn and Dikii (1966), and Dikii and Golitsyn (1968) studied these global oscillations theoretically. Ahlquist (1982, 1985) and Weber and Madden (1993) used daily observational data and projected global tropospheric analyses of geopotential height and velocity onto idealized three-dimensional, normal-mode Rossby wave structures. The climatology of these waves was studied and observations were compared with theoretical results. A review paper on large-scale traveling Rossby waves in the atmosphere was published by Madden (1979).

Eubanks et al. (1988) analyzed accurate geodetic data and found that rapid motions of the earth's pole exist and are significantly correlated with harmonic global-scale changes in the surface air pressure. They found that these changes are related to some of the longest

* The National Center for Atmospheric Research is sponsored by the National Science Foundation.

Corresponding author address: Dr. Harald Lejenäs, Department of Meteorology, Stockholm University, 106 91 Stockholm, Sweden.
E-mail: harald@misu.su.se

observed normal modes (with zonal wavenumber 1) and that one of these modes is the 16-day wave.

In the present study we investigate the impact of planetary-scale free Rossby waves on the component of atmospheric angular velocity parallel to the earth's rotational axis. These waves propagate toward the west. Pressure torques varying in time then arise as a consequence of unequal pressure on the eastern and western sides of mountains and small-scale topographic features. These torques are referred to as mountain torques. The angular momentum balance equation integrated over the entire atmosphere reads (compare, for instance, Boer 1990):

$$\frac{dM}{dt} = T_m + T_S, \tag{1}$$

where M is atmospheric angular momentum, that is, the sum of omega momentum and relative momentum. The torques on the right-hand side are mountain torques (T_m) and stress torques (T_s). Stress torques are principally caused by surface friction. In the present study we compute the contribution to the rate of change of M caused by mountain torques created by various free planetary-scale Rossby waves. Mountain torques are estimated from (see, for instance, Boer 1990):

$$T_m = -\int_0^{2\pi}\int_{-\pi/2}^{\pi/2} a^2 \cos\phi p_s \frac{\partial H}{\partial \lambda}\, d\phi\, d\lambda, \tag{2}$$

where p_s is the surface pressure, H the height of the earth's surface, λ the longitude, and ϕ the latitude.

The paper is organized as follows. In section 2 the theory for idealized normal-mode Rossby wave structures is recapitulated. In section 3 we discuss the evaluation of mountain torques. The contribution from all global-scale Rossby waves under study to the rate of change of atmospheric angular momentum is discussed in section 4. Finally, concluding remarks are found in section 5.

2. Theory

According to linear theory, normal-mode Rossby waves in an atmosphere at rest have horizontal structures described by Hough functions (Longuet-Higgins 1968; Kasahara 1976). In an isothermal atmosphere they have the vertical structure of a Lamb wave (Lamb 1932). In the presence of more realistic basic states, structures and frequencies of the normal modes differ somewhat from those with a basic state at rest (Salby 1981a,b). Golitsyn and Dikii (1966) and Dikii and Golitsyn (1968) showed that for large scales the height field is approximately proportional to some linear combination of associated Legendre polynomials. Haurwitz (1940) used the nondivergent vorticity equation on a sphere to study free global-scale Rossby waves. He showed that the latitudinal dependence, $p(\theta)$, of the pressure field associated with the (n, m) wave is given by

$$p(\theta) = \frac{n+1}{n}\sin\phi P_n^m(\cos\theta) - \frac{n-m+1}{n(n+1)}P_{n+1}^m(\cos\theta). \tag{3}$$

Here θ is the colatitude and P_n^m an associated Legendre polynomial of order m and degree n. The left-hand side, $p(\theta)$, is thus a dimensionless number ranging from -1 to $+1$. Further,

$$P_n^m(\cos\theta) = (1 - \cos^2\theta)^{m/2}\frac{d^m}{dx^m}[P_l(\cos\theta)], \tag{4}$$

where $P_l(\cos\theta)$ is a Legendre polynomial. Expression (3) is a very close approximation of the large-scale Hough functions. We will use (3) to describe the horizontal structures of the pressure fields associated with each wave, and we refer to two observation papers to decide on what waves we should consider. Ahlquist (1982) used three years of National Centers for Environmental Prediction (formerly the National Meteorological Center) twice daily data from 1 July 1976 to 13 October 1979 and estimated approximate periods and computed the waves' pressure amplitude where the amplitude is largest (his Table 3). Weber and Madden (1993) used 10 years of global tropospheric European Centre for Medium-Range Weather Forecasts data (1 December 1978–31 December 1988) for a similar study. They projected Rossby waves onto Hough normal modes by seasons to identify presence of these waves during the four seasons (their Table 1).

The latitudinal structure of the pressure perturbations for some waves were presented by Weber and Madden (1993). Ahlquist (1982) showed schematic views of the global geopotential and velocity fields for two of these waves (his Fig. 2). We computed the latitudinal structure of the pressure perturbations for all waves identified by Ahlquist and Weber and Madden using Eq. (3). For the sake of completeness, they are reproduced in Fig. 1. The maximum amplitude is normalized to 1.

3. Mountain torques

a. Evaluation and normalized data

Madden (1979) plotted the amplitude as a function of height of the 5-day wave, that is, $m = 1$, $n - m = 1$ at 30°N during the summer (his Fig. 8), and the 16-day wave, that is, $m = 1$, $n - m = 3$ at 60°N during the winter (his Fig. 9). There is a slight increase with height of the amplitude of the geopotential height for these two waves reminiscent of the Lamb wave vertical structure. To compute mountain torques we need to know the perturbation pressure at the earth's surface. We considered all waves in Fig. 1 to be amplitudes (in hPa) at sea level. Further, we assumed that the pressure perturbations vary with height as a Lamb wave. Gill (1982) showed that for such a wave, pressure varies with height as

$$p(z) = p_s \exp(-z/H_s), \tag{5}$$

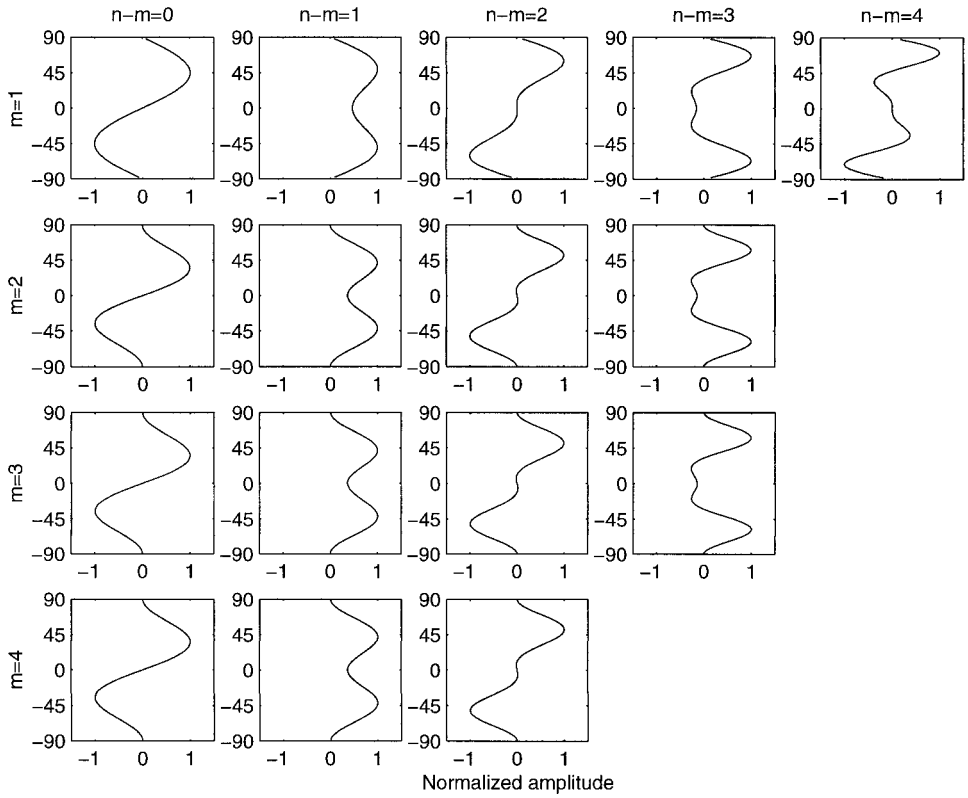

FIG. 1. The latitudinal structure of the pressure perturbations for all Hough normal modes. Here, m is the zonal wavenumber, and n the meridional wavenumber. The amplitude is normalized to 1.

where p_s is the pressure at sea level; z is the height above sea level; and H_s is the scale height, that is, the height at which the pressure has fallen to e^{-1} of its surface value. The scale height for an isothermal atmosphere is

$$H_s = \frac{RT}{g}. \tag{6}$$

For the temperature we used $T = 273$ K, so H_s is 8.0 km. We then consider p (at $z = H$), or the perturbation pressure at the earth's surface, to be given by (5). Salby (1979) has shown that this so-called Lamb structure is only weakly affected when a realistic temperature profile is substituted for an isothermal one. For the stratosphere, which we do not consider here, dissipation may play an important role in altering the vertical structure (Salby 1980).

Mountain torques as a function of time caused by the waves pictured in Fig. 1 as they travel westward are plotted in Fig. 2. The variation in time of T_m was obtained by moving each pressure map, with the appropriate latitudinal structure of Fig. 1 and the longitudinal wavenumber m, westward, simulating its westward propagation. We used the T42 grid and shifted westward two grid points or 5.625° west each time step. This results in 64 time steps for a complete revolution around the earth. The length of a time step is determined from the period of the wave, which is plotted for each wave in the upper right corner (in days). Note that the periods in Fig. 2 are for an atmosphere with no background wind. We adopted the same orography as in the National Center for Atmospheric Research (NCAR) Community Climate Model (CCM3) model (NCAR 1998). The number of grid points the ridge has moved westward is plotted on the horizontal axes in Fig. 2. Note that for all waves the first value was obtained by positioning the ridge at Greenwich (0° or 360°). The ridge then made a complete revolution around the earth. It means that for zonal wavenumber 2 ($m = 2$) there are two identical parts (360°–180°, and 180°–0°, respectively). In the same way there are three identical parts for zonal wavenumber 3, and four for wavenumber 4. In Fig. 2 the full lines represent global mountain torque values, whereas dashed lines refer to the Southern Hemisphere, and dash-dotted lines to the Northern Hemisphere.

To test how sensible our assumption about the vertical variation of pressure perturbations is, we also computed mountain torques for pressure perturbations that are constant with height. These T_m values (not shown here) turned out to be almost identical to those in Fig. 2. Thus, for the planetary-scale free Rossby waves we study, the variation of the pressure perturbations with height is of little importance to our results.

The maximum T_m values in Fig. 2 vary considerably.

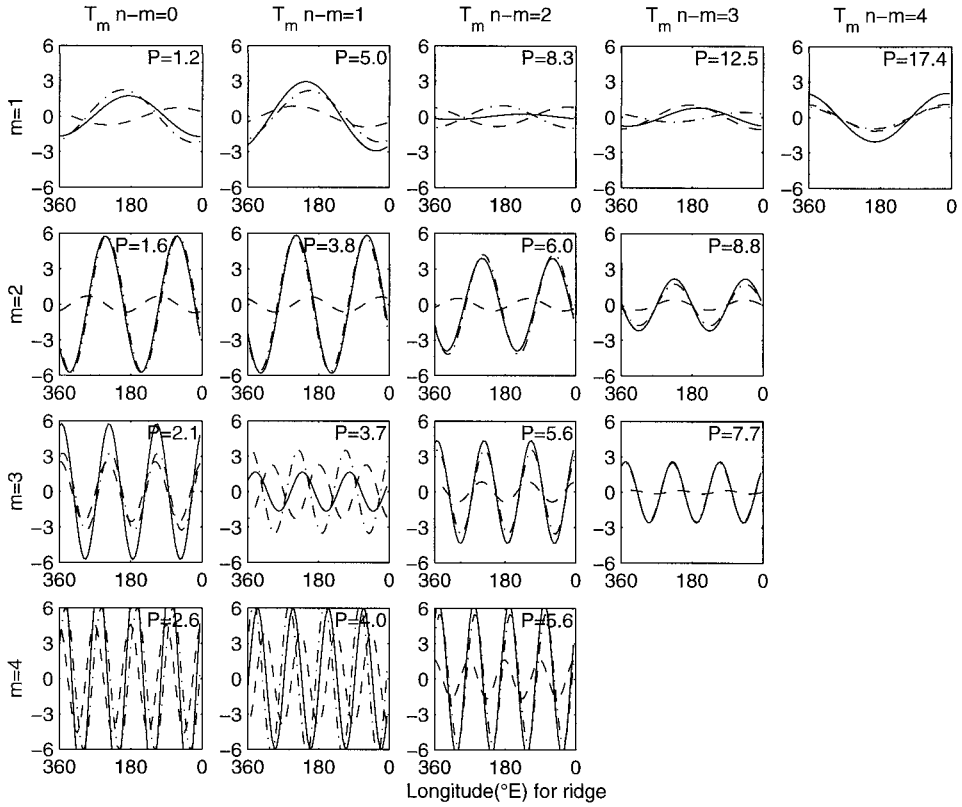

FIG. 2. Mountain torques as a function of time caused by Hough normal modes pictured in Fig. 1. Full lines show global mountain torque values; dashed lines refer to the Southern Hemisphere; and dash-dotted lines to the Northern Hemisphere. Values on the *x* axes show the position of the ridge during one complete revolution around the earth. Each ridge is positioned at Greenwich when the revolution starts, and all waves move westward. Periods (in days) are given in the upper right corner for each wave. The amplitude is 1 hPa for all waves. The unit for T_m is Hadleys (1 Hadley = 10^{18} kg m^2 s^{-2}).

At most they amount to 9 Hadleys (1 Hadley = 10^{18} kg m^2 s^{-2}). The better the orography projects onto the respective Rossby wave described by (3), the larger maximum values for T_m can be expected. Approximate maximum mountain torque values for each zonal wavenumber are

$m = 1,\ n - m = 1$ 3 Hadleys,
$m = 2,\ n - m = 0, 1$ 6 Hadleys,
$m = 3,\ n - m = 0$ 6 Hadleys, and
$m = 4,\ n - m = 0$ 9 Hadleys.

Since our treatment is a linear process, the normalized values of Fig. 2 can be converted to values of any amplitude by multiplying values in Fig. 2 by a given wave amplitude.

b. Observational data

The results presented in Fig. 2 are normalized in the sense that the amplitude of all waves is 1 hPa. In the real atmosphere it is, of course, not the same for all waves. We adopted the amplitudes found by Ahlquist (1982) to obtain realistic mountain torque values. The resulting torques as a function of time are shown in Fig. 3. We should point out that realistic winds, while apparently not drastically altering the structure of the waves in the troposhere, alter the periods. For example, the 1, 2 and 1, 3 ($m, n - m$) modes have actual periods near 10 and 16 days. In the extreme, a resonant wave with infinite period would contribute to a constant torque.

Observed amplitudes are plotted in the lower right corner (in hPa). As before, the ridge of the respective wave was positioned at Greenwich when the wave started its revolution around the earth. The maximum mountain torque values for each zonal wavenumber are

$m = 1,\ n - m = 3$ 1.5 Hadleys,
$m = 2,\ n - m = 2$ 2.3 Hadleys,
$m = 3,\ n - m = 2$ 2.6 Hadleys, and
$m = 4,\ n - m = 1$ 1.8 Hadleys.

Considering all meridional wavenumbers, zonal wavenumber 2 causes the largest global T_m values. The contribution from individual waves is close to 2 Hadleys,

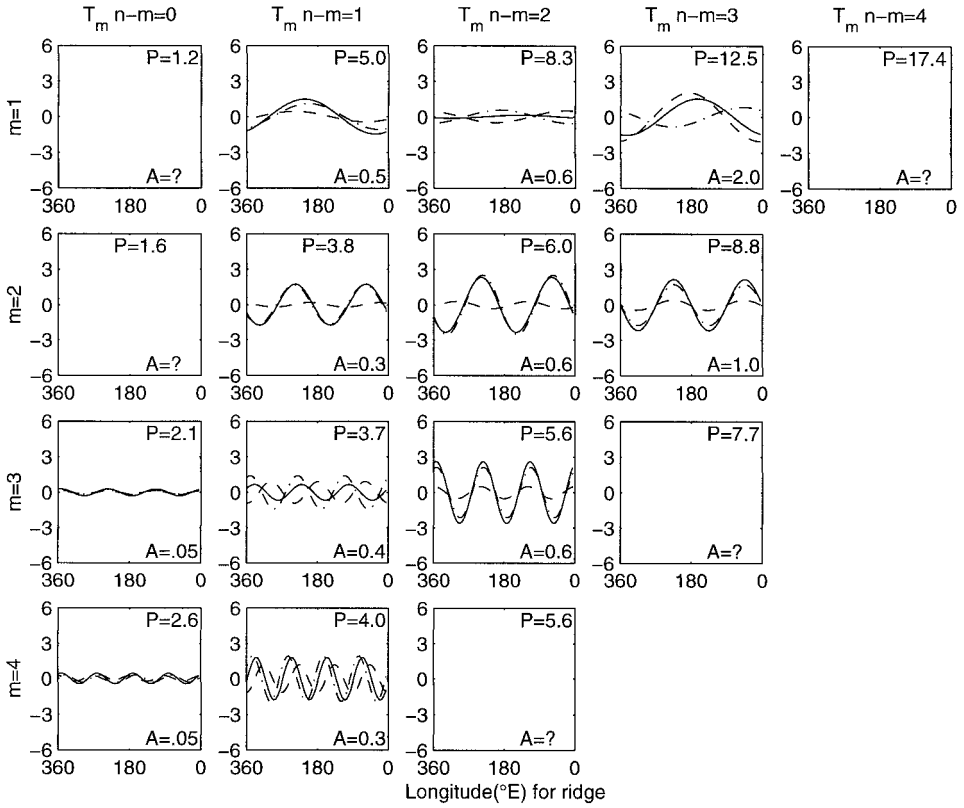

FIG. 3. Mountain torques as a function of time caused by Hough normal modes pictured in Fig. 1. Full lines show global mountain torque values, dashed lines refer to the Southern Hemisphere, and dash-dotted lines to the Northern Hemisphere. Values on the *x* axes show the position of the ridge during one complete revolution around the earth. Each ridge is positioned at Greenwich when the revolution starts, and all waves move westward. Periods (in days) are given in the upper right corner for each wave. Amplitudes are observed amplitudes as found by Ahlquist (1982). They are given (in hPa) in the lower right corner of each panel. The unit for T_m is Hadleys (1 Hadley = 10^{18} kg m^2 s^{-2}).

and the contribution comes almost entirely from the Northern Hemisphere. For most of the waves, the major contribution to T_m comes from the Northern Hemisphere. Other outstanding values are caused by the wave $m = 1$, $n - m = 3$ (1.5 Hadleys), which is the 16-day wave; the wave $m = 3$, $n - m = 2$ (2.6 Hadleys); and the wave $m = 4$, $n - m = 1$ (1.8 Hadleys). This compares with an observed semiannual amplitude ranging from 5 to 10 Hadleys (see Fig. 6 of Madden and Speth 1995), and subseasonal variations that often exceed 40 Hadleys (Figs. 3 and 10 of Madden and Speth 1995). It also compares with a semidiurnal amplitude of T_m of about 5 Hadleys resulting from the westward migration of the semidiurnal pressure wave (Madden et al. 1998). The semidiurnal pressure wave has a maximum amplitude of 2 hPa at the equator. Thus, mountain torques caused by these average-amplitude waves are of the same order as mountain torques caused by the semidiurnal pressure wave.

4. Exchange of angular momentum

By themselves, the varying mountain torques caused by the normal-mode global Rossby waves would exchange angular momentum between the atmosphere and the earth [cf. Eq. (1)]. We computed the contribution from T_m to the rate of change of total atmospheric angular momentum for each wave. The resulting angular momentum anomalies obtained by integrating the solid (global) torques in Fig. 3 over time are shown in Fig. 4. Also in this case the ridge was positioned at Greenwich, and then it moved two grid points westward each time step, all together one complete revolution around the earth (64 time steps). Naturally, the exchange of momentum is most pronounced for those waves that cause the largest mountain torques and/or have the longest periods. The period (in days) for each wave is given in the upper right corner of each panel in Fig. 4, and the amplitude (in hPa) is given in the lower right corner. The values of the amplitudes in Fig. 4 are observed values; however, they are averaged values. Zonal wavenumbers 1 and 2 cause the largest momentum anomalies. The maximum peak-to-trough amplitude for the average-amplitude waves of Ahlquist (1982) is 4.9×10^{23} kg m^2 s^{-1}, and it is caused by the 16-day wave ($m = 1$, $n - m = 3$). For zonal wavenumber 2, the maximum peak-to-trough momentum amplitudes are $2.4 \times$

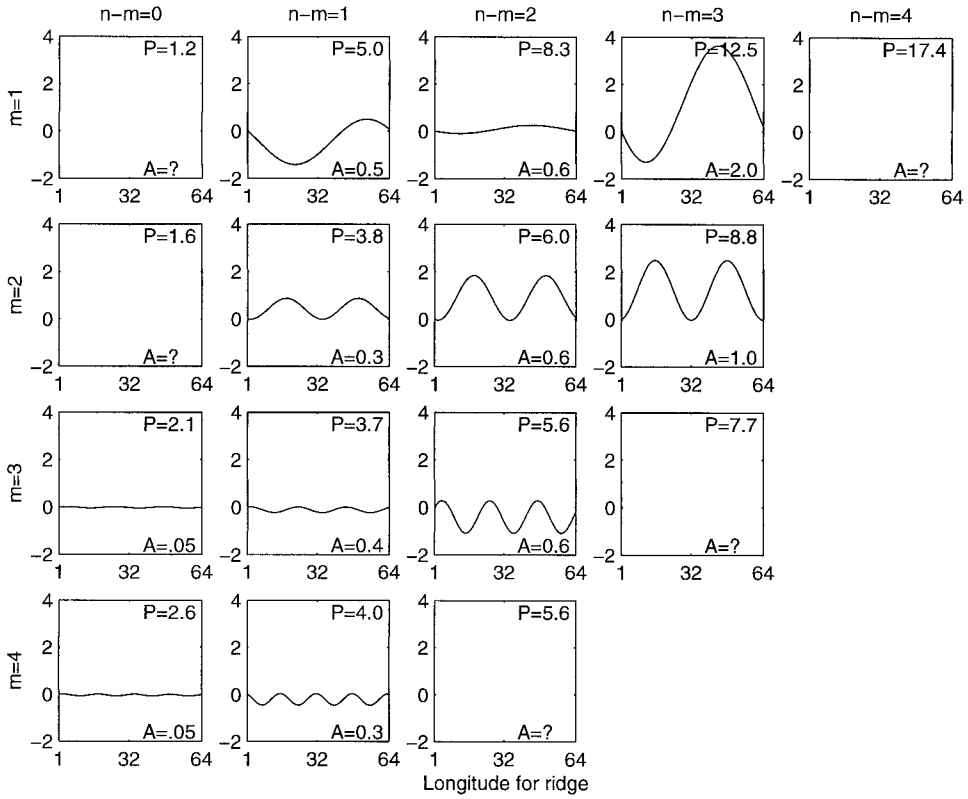

FIG. 4. Anomaly atmospheric angular momentum caused by mountain torques for all waves in Fig. 3. The values are global values obtained by integrating the solid (global) torques in Fig. 3. The unit is 10^{23} kg m^2 s^{-1}.

10^{23} (for $n - m = 2$) and 1.9×10^{23} (for $n - m = 3$). For zonal wavenumber 3, it is only one wave that causes large momentum amplitudes, that is, $n - m = 2$, and the peak-to-trough amplitude as 1.1×10^{23}. Wavenumber 4 causes only small anomalies. All these angular momentum anomaly values compare with observed subseasonal variations of up to 40×10^{24} kg m^2 s^{-1} (Fig. 9 of Madden and Speth 1995), so that the contribution of Rossby waves with average amplitudes, at least, are two orders of magnitude smaller. Individual waves may have bigger amplitudes. For instance, Madden and Labitzke (1981) studied a pronounced 16-day wave during January 1979, and according to their Fig. 3, the amplitude of the wave is near 100 gpm at 850 hPa, which would translate to a pressure amplitude of 8–10 hPa or a peak-to-trough momentum anomaly of $20–25 \times 10^{23}$ kg m^2 s^{-1}.

5. Summary

Normal-mode planetary-scale Rossby waves in the earth's atmosphere propagate westward. They are associated with pressure perturbations that also move westward. Pressure torques varying in time then arise as a consequence of unequal pressure on the eastern and western sides of mountains and small-scale topographic features. We have studied these mountain torques. Comparing contributions from individual waves, we found that for the average wave amplitudes the maximum torque for a particular wave is around 2 Hadleys, and that considering all meridional wavenumbers, zonal wavenumber 2 causes the largest global torques. These torques are small compared to subseasonal variations. They are, however, of the same order of magnitude as mountain torques caused by the semidiurnal pressure wave studied by Madden et al. (1998).

The mountain torques cause angular momentum anomalies. Changes in angular momentum depend on both the amplitude of the changing torque and its period. As a result, zonal wavenumbers 1 and 2 cause the largest peak-to-trough amplitudes, $2–5 \times 10^{23}$ kg m^2 s^{-1}. The 16-day wave ($m = 1$, $n - m = 3$) produces the largest amplitude, 4.9×10^{23} kg m^2 s^{-1}. Again, these values refer to Rossby waves with average amplitudes reported in the literature. These fluctuations amount to roughly 1% of observed subseasonal variations in atmospheric angular momentum, which means that they are almost irrelevant to observed subseasonal variations. Individual waves, in particular the 16-day wave, may cause momentum anomalies up to 5 times as big.

Acknowledgments. Part of this work was done while

the second author was a visitor to the International Meteorological Institute in Stockholm. J. Tribbia is acknowledged for discussions about the vertical structure of free Rossby waves. Comments from three anonymous reviewers helped to improve the paper.

REFERENCES

Ahlquist, J. E., 1982: Normal-mode global Rossby waves: Theory and observations. *J. Atmos. Sci.,* **39,** 193–202.

——, 1985: Climatology of normal mode Rossby waves. *J. Atmos. Sci.,* **42,** 2059–2068.

Boer, G. J., 1990: Earth–atmosphere exchange of angular momentum simulated in a general circulation model and implications for the length of day. *J. Geophys. Res.,* **95,** 5511–5531.

Deland, R. J., 1964: Traveling planetary waves. *Tellus,* **16,** 271–273.

——, and Y. J. Lin, 1967: On the movement and prediction of planetary-scale waves. *Mon. Wea. Rev.,* **95,** 21–31.

Dikii, L. A., 1965: The terrestrial atmosphere as an oscillating system. *Izv. Akad. Nauk SSSR, Atmos. Oceanic Phys.,* **1,** 469–489.

——, and G. Golitsyn, 1968: Calculations of the Rossby wave velocities in the Earth's atmosphere. *Tellus,* **20,** 314–317.

Eliasen, E., and B. Machenhauer, 1965: A study of the fluctuations of atmospheric planetary flow patterns represented by spherical harmonics. *Tellus,* **17,** 220–238.

Eubanks, T. M., J. A. Steppe, J. O. Dickey, R. D. Rosen, and D. A. Salstein, 1988: Causes of rapid motions of the Earth's pole. *Nature,* **334,** 115–119.

Gill, A. E., 1982: *Atmosphere–Ocean Dynamics.* Academic Press, 662 pp.

Golitsyn, G., and L. A. Dikii, 1966: Oscillations of planetary atmospheres as a function of the rotational speed of the planet. *Izv. Akad. Nauk SSSR, Atmos. Oceanic Phys.,* **2,** 225–235.

Haurwitz, B., 1940: The motion of atmospheric disturbances on the spherical earth. *J. Mar. Res.,* **3,** 254–267.

Hough, S. S., 1898: On the application of harmonic analysis to the dynamical theory of tides. II: On the general integration of Laplace's dynamical equations. *Philos. Trans. Roy. Soc. London* **191A,** 139–185.

Kasahara, A., 1976: Normal modes of ultralong waves in the atmosphere. *Mon. Wea. Rev.,* **104,** 669–690.

Lamb, H., 1932: *Hydrodynamics.* Dover, 738 pp.

Lounguet-Higgins, F. R. S., 1968: The eigenfunctions of Laplace's tidal equations over a sphere. *Philos. Trans. Roy. Soc. London* **262A,** 511–607.

Madden, R. A., 1978: Further evidence of traveling planetary waves. *J. Atmos. Sci.,* **35,** 1605–1618.

——, 1979: Observations of large-scale traveling Rossby waves. *Rev. Geophys. Space. Phys.,* **17,** 1935–1949.

——, and P. R. Julian, 1972: Further evidence of global-scale 5-day pressure waves. *J. Atmos. Sci.,* **29,** 1464–1469.

——, and J. Stokes, 1975: Evidence of global-scale 5-day waves in a 73-year pressure record. *J. Atmos. Sci.,* **32,** 831–836.

——, and K. Labitzke, 1981: A free Rossby wave in the troposphere and stratosphere during January 1979. *J. Geophys. Res.,* **86** (C2), 1247–1254.

——, and P. Speth, 1995: Estimates of angular momentum, friction, and mountain torques during 1987–1988. *J. Atmos. Sci.,* **52,** 3681–3694.

——, H. Lejenäs, and J. J. Hack, 1998: Semidiurnal variations in the budget of angular momentum in a general circulation model and in the real atmosphere. *J. Atmos. Sci.,* **55,** 2561–2575.

NCAR, cited 1998: U.S. Navy Global Elevation Data, 10-min (1984 DEC). [Available online at http://goldhill.cgd.ucar.edu/cms/ccm3/initial/topo.README.]

Salby, M. L., 1979: On the solution of the homogeneous vertical structure problem for long-period oscillations. *J. Atmos. Sci.,* **36,** 2350–2359.

——, 1980: The influence of realistic dissipation on planetary normal structures. *J. Atmos. Sci.,* **37,** 2186—2199.

——, 1981a: Rossby normal modes in nonuniform background configurations. Part I: Simple fields. *J. Atmos. Sci.,* **38,** 1803–1826.

——, 1981b: Rossby normal modes in nonuniform background configurations. Part II: Equinox and solstice conditions. *J. Atmos. Sci.,* **38,** 1827–1840.

Weber, R. O., and R. A. Madden, 1993: Evidence of traveling external Rossby waves in the ECMWF analyses. *J. Atmos. Sci.,* **50,** 2994–3007.